JOURNAL OF MATERIALS SCIENCE 28 (1993) 3049–3058

Si–C–N ceramics with a high microstructural stability elaborated from the pyrolysis of new polycarbosilazane precursors

Part IV *Oxygen-free model monofilaments*

D. MOCAER, R. PAILLER, R. NASLAIN
Laboratoire des Composites Thermostructuraux (UMR 47 CNRS-SEP-UB1), Domaine Universitaire, 3 Allée de la Boëtie, F 33600 Pessac, France

C. RICHARD, J. P. PILLOT, J. DUNOGUES
Laboratoire de Chimie Organique et Organométallique (URA 35 CNRS), Université Bordeaux I, 351 Cours de la Libération, F 33405 Talence, France

C. DARNEZ
Commissariat à l'Energie Atomique, Centre d'Etudes du Ripault, F 37260 Monts, France

M. CHAMBON, M. LAHAYE
CUMENSE, Université Bordeaux I, 351 Cours de la Libération, F 33405 Talence, France

Si–C–N model filaments almost free of oxygen have been prepared from a novel PCSZ precursor by melt-spinning, γ-ray curing and pyrolysis under pure nitrogen (or argon) at a temperature θ_p as high as 1600 °C. The organic–inorganic conversion of the precursor takes place at $450 < \theta_p < 850$ °C. It yields an amorphous filament whose composition is close to $SiC_{0.93}N_{0.46}$ (with less than 2 wt % O). No significant change in composition and microstructure occurs up to about 1400 °C. Beyond 1400 °C under argon, a decomposition process takes place starting from the filament surface whereas, under nitrogen, the only observed phenomena are the growth of a skin a few nanometres thick at the filament surface and the formation of tiny β-SiC crystals within the amorphous Si–C–N material. As θ_p is raised, the Young's modulus at room temperature continuously increases to reach a value close to 220 GPa for $\theta_p = 1600$ °C whereas the tensile failure stress undergoes a broad maximum close to 2400 MPa for $\theta_p = 1200$ °C and is still higher than 2000 MPa after ageing at 1600 °C. Thus, Si–C–N filaments free of oxygen have improved stability at high temperatures with respect to Si–C–O filaments processed under similar conditions.

1. Introduction

The potential of metal-matrix composites (MMC) [1–3] and ceramic-matrix composites (CMC) [3–6] as structural materials for applications at high temperatures (e.g. in the aerospace industry field) is limited, among others, by the poor high-temperature characteristics of the reinforcements presently available. Oxide-based fibres such as alumina [7–9] and zirconia [10] fibres are chemically very stable at high temperatures, with respect to atmospheres containing oxygen. Unfortunately, they undergo grain growth phenomena even at medium temperatures which lower their failure strength. Conversely, carbon fibres are known to exhibit a good microstructural stability and excellent mechanical properties at high temperatures but they are very sensitive to oxygen even at temperatures as low as 500–600 °C [11, 12].

A variety of fibres, referred to as SiC [13–23] or Si_3N_4 [24–26] fibres, amorphous or microcrystalline, have been elaborated from organosilicon precursors according to a spinning–curing–pyrolysis procedure similar to that previously used for the carbon fibres. Since both SiC and Si_3N_4 exhibit an excellent resistance to oxidation (related to the growth of a thin protective scale of silica: the so-called passive oxidation regime), up to 1500–1600 °C, one could expect that SiC (or Si_3N_4) fibres were among the best materials for the reinforcement of CMCs. This is actually true as long as the temperature does not exceed about 1200 °C. Beyond this temperature, their microstructure is no longer stable owing to the occurrence of a large amount of oxygen (i.e. 10–20 wt %) in their composition. Oxygen is mainly picked up by the green fibre during the curing process (the organosilicon precursor is usually spun in the molten state and it is made unmeltable by an oxidation process) and remains in the amorphous state after pyrolysis (owing to the stability of the Si–O bond) [27]. Only when the

0022–2461

temperature is raised beyond about 1200 °C (for the Si–C–O fibres) is oxygen released as SiO and CO [27–29]. Unfortunately, this decomposition, which proceeds radially from the external surface of the fibre, has two negative consequences: (i) it yields, with an important diameter shrinkage and weight loss, a β-SiC + C mixture in which the β-SiC crystal size increases as the temperature is raised and (ii) it results in a dramatic drop in both the tensile failure strength and stiffness [18, 19]. Conversely, this decomposition process, which takes place at a temperature corresponding roughly to the CMC processing conditions, is also responsible for the formation of a thin layer of carbon at the fibre surface, acting as an interphase or mechanical fuse in the composites. Therefore, the non-brittle behaviour of SiC glass–ceramic or SiC–SiC composites is at least partly a beneficial consequence of the low thermal stability of oxygen-cured ex-organosilicon fibres [30–32].

Since it has been established that the use at high temperatures of ex-organosilicon fibres was actually limited by the oxygen introduced in the material during the curing step, attempts have been made to lower the oxygen concentration or better to select curing processes which did not involve oxygen. Si–C–N(O) fibres (HPZ fibres from Dow Corning) containing only a few per cent of oxygen have been obtained from hydridopolysilazane (HPZ) precursors utilizing a curing process with $HSiCl_3$ (instead of water vapour used previously) [33]. Independently, Si–C–N(O) fibres (Fiberamic from Rhône-Poulenc) with a rather low oxygen content (8 wt %) have been prepared by spinning a polysilazane (PSZ) and making the fibres obtained unmeltable by thermal and chemical curing [34]. Finally, ex-polycarbosilane (PCS) fibres, almost free of oxygen (0.4 wt %), have been very recently elaborated utilizing a physical curing process (electron beam curing) and were reported to exhibit a drop in their room-temperature mechanical characteristics after an ageing treatment of 1 h at 1500 °C [35, 36].

The present contribution is part of work devoted to a new polycarbosilazane (PCSZ) precursor and to the related Si–C–N and Si–C–N–O ceramics. Previous articles published on the subject (parts 1–3) dealt with (i) the synthesis of the precursor and its conversion by pyrolysis into bulk Si–C–N ceramic samples [37], (ii) its curing by oxygen [38] and (iii) the preparation and pyrolysis of oxygen-cured PCSZ model monofilaments [39]. It has thereby been shown that oxygen-cured PCSZ filaments remain amorphous within a wide range of temperatures (i.e. from 850 to about 1400 °C) under an argon or nitrogen atmosphere. Beyond 1400 °C, the filaments undergo a decomposition–crystallization or a decomposition–nitriding process depending on whether the pyrolysis is performed under argon or nitrogen, respectively. The heteroatoms (N and O) were shown to impede the growth of β-SiC crystals. The effect of both pyrolysis temperature and atmosphere on the room-temperature failure strength and stiffness was discussed.

The aim of the present contribution is (i) to discuss the preparation and properties of oxygen-free Si–C–N model monofilaments which have been spun from molten PCSZ precursor, cured with γ-rays and pyrolysed under argon or nitrogen; and thus, by comparison with the data previously presented in part III [39], (ii) to show the effect of oxygen on their microstructure and mechanical properties at room temperature.

2. Experimental procedure

2.1. Preparation of the ex-PCSZ Si–C–N model filaments

The PCSZ precursor used in the present work was prepared according to a two-step process described in detail elsewhere [40]. In the first step, a polysilasilazane (PSSZ) was prepared by adding dimethyldichlorosilane and 1,3-dichloro-1,3-dimethyldisilazane, in equimolar ratio, to a suspension of sodium in boiling toluene. In a second step, the clear, mobile PSSZ was converted into crosslinked PCSZ by heating progressively at temperatures up to 400 °C under argon. Among other complex mechanisms, this pathway certainly involves methylene group insertions into Si–Si bonds as previously reported for disilanes and polysilanes [41, 13, 37]. At this stage, the average molecular weight $\bar{M}_w$ was about 15 200. The material, referred to as PCSZ-II in part 1 [37], corresponds to the formula $SiC_{1.22}N_{0.45}H_{4.2}O_{0.03}$, showing that the contamination by oxygen during processing has been very low.

The PCSZ precursor was spun, in the molten state, with a laboratory-scale apparatus equipped with a single spinneret, in order to prepare a continuous monofilament 25 μm in diameter. The green filament was then cut, in a glove box filled with a dry inert atmosphere, in a gauge of 50 mm length.

The green PCSZ filaments were cured with γ-rays under dry argon according to the following procedure: (i) they were first introduced, under the argon atmosphere of the glove-box, in aluminium containers subsequently tightly sealed, then (ii) the containers were set within the irradiation chamber of a ^{60}Co source and submitted to an overall irradiation dose ranging from 50 to 350 Mrad (the irradiation rate being close to 0.5 Mrad h^{-1}) and finally (iii) the irradiated containers were opened in the glove box in order to avoid any contact with oxygen and moisture during the curing step.

The γ-ray cured filaments were set in a boat of silica, transferred to a pyrolysis furnace whose glass silica tube was directly connected to the glove box, and pyrolysed in an atmosphere of argon (P = 100 kPa) up to 850 °C (heating rate: 50 °C h^{-1}; plateau at 850 °C: 15 min). After such treatment, which corresponds basically to the organic–inorganic transition as discussed in parts I–III [37–39], the material is no longer sensitive to oxygen and moisture. The pyrolysis, performed under pure nitrogen or argon, was achieved with high-temperature pyrolysis equipment (r.f. heating), according to a procedure described in part I [37], up to a value θ_p (the material being maintained for 15 min at θ_p). The flow chart of the overall process is shown in Fig. 1.

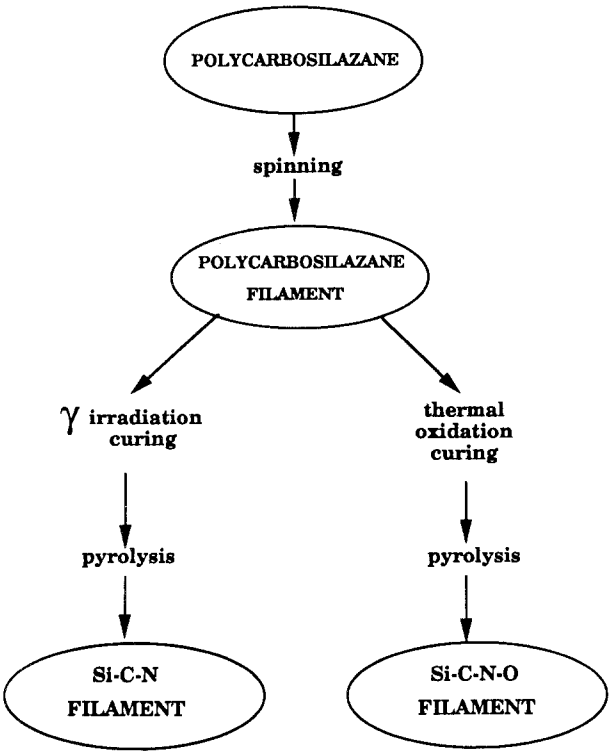

Figure 1 Flow chart of the process used to prepare the Si–C–N (present work) and Si–C–N–O (part III [39]) filaments from the same PCSZ-II precursor.

2.2. Characterization of the filaments

The elemental analyses and mechanical tests performed on Si–C–N filaments after the γ-ray curing and pyrolysis steps have been previously described in parts I–III [37–39] and will be only briefly recalled for the purpose of the discussion.

The measurement of the insoluble fraction was performed on filaments submitted to increasing dose of γ-rays, as follows: a sample (mass m_0) of filaments was treated with hexane at 25 °C for 15 min and the resulting solution filtered. The solid residue was dried at 150 °C and its mass m_s was measured. The insoluble fraction in hexane τ_i was calculated as $\tau_i = m_s/m_0$.

In order to study the effect of the γ-ray irradiation dose on the weight loss during pyrolysis, thermogravimetric analysis (TGA) (TGS 2 apparatus from Perkin Elmer) was performed up to 950 °C under an argon atmosphere (P = 100 kPa) up to 950 °C (heating rate: 300 °C h^{-1}), the sample (m_0 = 10 mg) being set in a platinum crucible.

Elemental analysis was performed by electron probe microanalysis (EPMA) (Camebax 75 from Cameca) from polished cross-sections of the filaments utilizing two different monochromators (i.e. PET for SiK_α and a multilayer PCI pseudo-crystal for CK_α, OK_α and NK_α) and pure SiC, BN and SiO_2 as standards. Auger depth–concentration profiles were recorded from the filament surface by Auger electron spectroscopy (AES) (scanning Auger microprobe PHI-590 from Perkin-Elmer) with an Ar^+ sputtering gun. The apparent atomic concentrations were derived from the intensities of the Si*LVV*, C*KLL*, O*KLL* and N*KLL* Auger electron transitions, utilizing the derivative mode. It should be emphasized that (i) these concentration measurements are only semi-quantitative and (ii) the sputtered depths that will be mentioned in the following are only relative values (reference : Ta_2O_5 sputtering rate), the actual sputtering rate for the Si–C–N filaments being unknown.

Transmission electron microscopy (TEM) was performed (2000 FX TEM from Jeol) on thin sections of filament obtained by ultramicrotomic according to the bright-field, dark-field and selected-area diffraction (SAD) modes. The dark-field images were recorded by setting the aperture in position 2, i.e. it was centred at 4.2 nm^{-1} in order to select, among others, the 1 1 1 reflection of β-SiC. Scanning electron microscopy (SEM) (840 SEM from Jeol) was used to observe the filament surface and assess the morphology of the tensile failure surfaces.

Finally, the ex-PCSZ Si–C–N filaments were tensile tested at room temperature (gauge length L = 10 mm) with a microtensile tester similar to that described by Bunsell *et al.* [42]. The mean tensile failure stress σ^R was calculated from the data obtained from an average of 20 tests and the Young's modulus taken as the slope of the stress–strain curve at the origin.

3. Results

3.1. Insoluble fraction after γ-ray curing and weight loss during pyrolysis

The variation, as a function of the irradiation dose, of the fraction τ_i insoluble in hexane and the ceramic yield η after pyrolysis at θ_p = 950 °C are shown in Fig. 2. Both curves exhibit the same general features which can be presented as follows: (i) a sharp increase in both τ_i and η as the irradiation dose is raised to about 150 Mrad followed by (ii) a smooth increase in τ_i and η as the irradiation dose is raised up to 350 Mrad. The filaments which were cured with an irradiation dose of the order of 150 Mrad exhibit, after pyrolysis, a shrunken surface with many defects thought to be detrimental to the tensile failure stress, as shown in Fig. 3. Therefore, the effect of the pyrolysis temperature θ_p on the properties of the Si–C–N filaments (discussed in section 4 below) was studied on materials having received a γ-ray irradiation dose

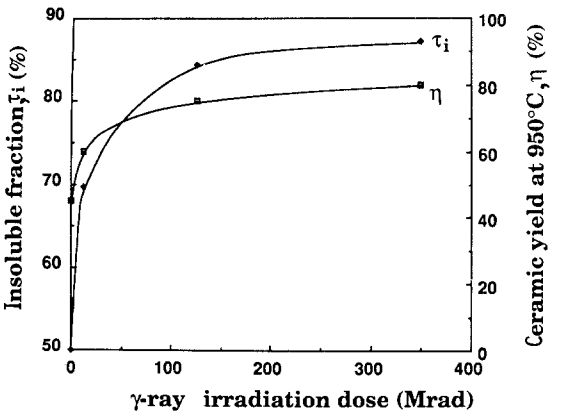

Figure 2 Variations, as a function of the γ-ray irradiation dose, of the insoluble fraction in hexane and ceramic yield at 950 °C of PCSZ model filaments.

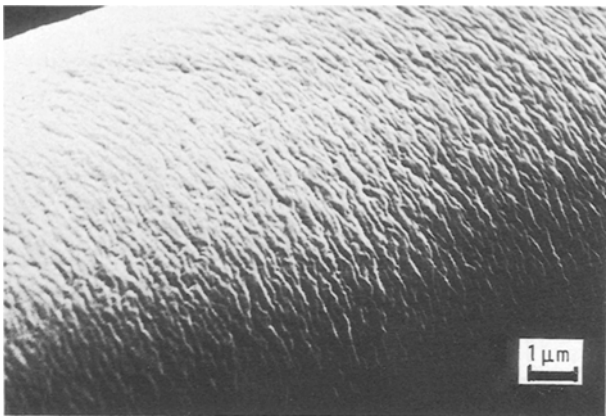

Figure 3 Surface morphology of Si–C–N filament after insufficient γ-ray curing (irradiation dose 150 Mrad) and pyrolysis treatment under nitrogen at 1200 °C.

equal to 350 Mrad (no attempt was made to establish the minimum irradiation dose resulting in no detrimental shrinkage after pyrolysis).

The variations of the weight loss $\Delta m/m_0$ as a function of temperature θ_p, before and during the organic–inorganic transition, are shown in Fig. 4 for both cured and uncured PCSZ-II filaments. The main difference between the two materials lies in the fact that the uncured PCSZ-II precursor has already undergone a weight loss of the order of 23% (compared with only 10% for the cured filaments) before the beginning of the organic–inorganic transition, i.e. within the temperature range 25–450 °C. As discussed in part I [37], this kind of weight loss has been assigned to an evolution of oligomers. On the other hand, the weight loss during the organic–inorganic transition itself (i.e. for $450 < \theta_p < 850$ °C) is almost the same, i.e of the order of 10%, for both materials. Thus, the overall weight loss for $\theta_p = 950$ °C is 33 and 20% for the uncured and cured PCSZ-II, respectively.

3.2. Chemical composition

The elemental compositions of ex-PCSZ-II γ-ray cured Si–C–N filaments after pyrolysis in an atmosphere of pure nitrogen at $\theta_p = 1000$, 1200, 1400 and 1600 °C are shown in Table I. It appears from the data that (i) the composition of the filaments remains unchanged when θ_p is raised: it corresponds to the formula $SiC_{0.93}N_{0.46}O_{0.05}$, and (ii) the oxygen concentration at the very end of the pyrolysis treatment is less than 2 wt %. Furthermore and as previously discussed in parts I and III [37, 39], hydrogen (which cannot be analysed by EPMA) might be present in small amounts, particularly for low θ_p values.

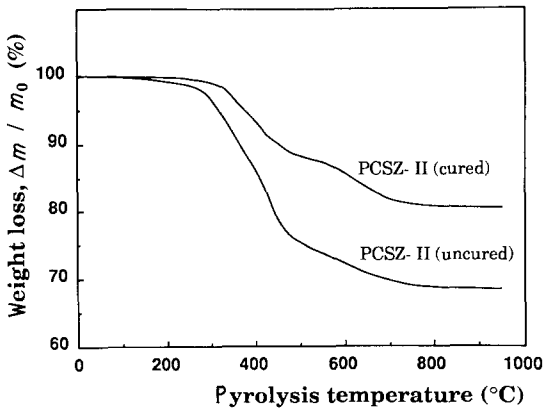

Figure 4 Variations of the weight loss, $\Delta m/m_0$, as a function of temperature before and during the organic–inorganic transition in cured and uncured PCSZ-II filaments.

It has been shown in part III that Si–C–N–O filaments prepared from the same PCSZ-II precursor but according to a procedure involving an oxygen curing step (see Fig. 1) underwent beyond $\theta_p = 1400$ °C either a decomposition–crystallization or decomposition–nitriding process (in argon and nitrogen, respectively) which started from the filament surface and moved radially towards the filament axis at a rate depending on θ_p [39]. In order to establish whether such processes occur in oxygen-free filaments, AES depth concentration profiles were recorded from the surface of filaments which had been submitted to a pyrolysis treatment at or beyond $\theta_p = 1400$ °C under either nitrogen or argon. The results are shown in Fig. 5.

For $\theta_p \leq 1400$ °C, the filaments heated under nitrogen do not exhibit any significant decomposition zone near their surface (Fig. 5a). The Si, C, N, O concentrations are homogeneous, at least to a first approximation, over the entire sputtered thickness and in good agreement with those measured by EPMA (Table I). The only noticeable feature is a small decrease in the silicon concentration in the very vicinity of the filament surface, which suggests that an evolution of silicon-containing gases might have occurred. For $\theta_p = 1600$ °C, a thin layer (i.e. 40–50 nm in apparent thickness) of a carbon-rich material has been formed at the filament surface during pyrolysis whereas the composition of the material below is still homogeneous and unchanged (Fig. 5b). Thus, it appears that the actual surface of Si–C–N filaments pyrolysed at 1600 °C under nitrogen consists of almost pure carbon.

The results are different with the filaments treated under argon. At $\theta_p = 1400$ °C the decomposition layer, although of similar apparent thickness (i.e. 50–60 nm), exhibits a different composition: (i) it is enriched in carbon and depleted in both N and O and (ii) the filament surface itself no longer consists of pure

TABLE I Chemical composition of ex-PCSZ γ-ray cured Si–C–N filaments pyrolysed under an atmosphere of nitrogen ($P = 100$ kPa) at increasing pyrolysis temperature, as established from EPMA data (hydrogen which might be present cannot be measured using this technique)

θ_p (°C)	Composition (at %)			
	Si	C	N	O
1000	41	38	19	2
1200	40	38	19	3
1400	41	38	19	2
1600	40	39	19	2

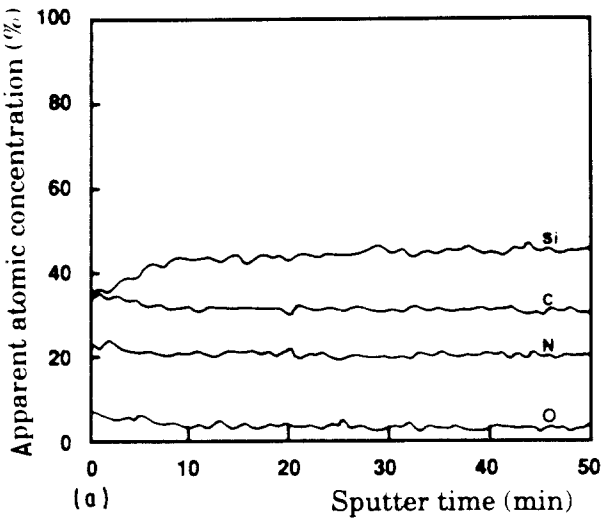

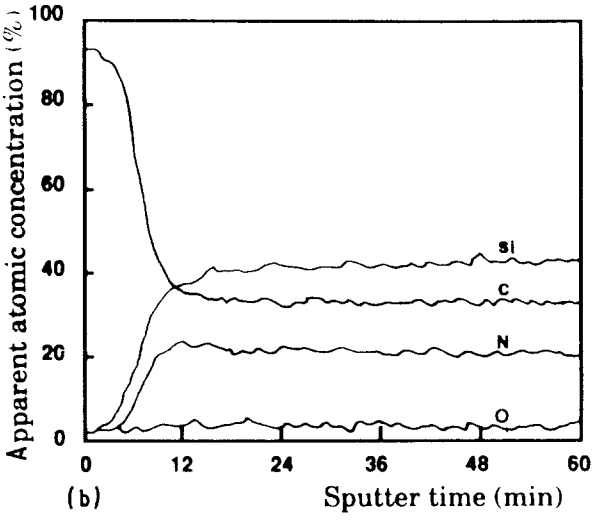

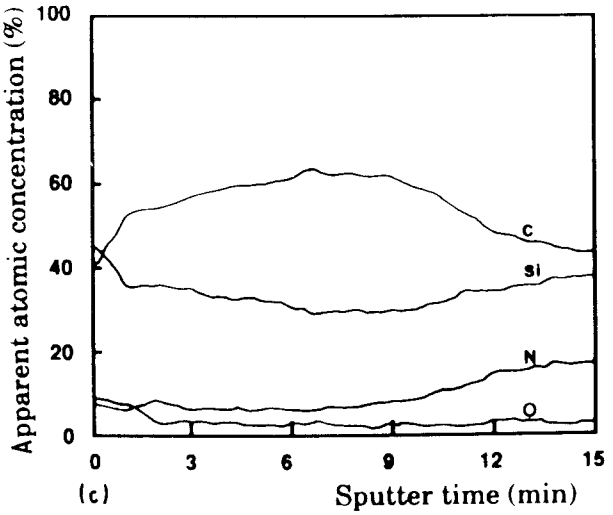

Figure 5 AES depth concentration profiles recorded radially from the surface for ex-PCSZ-II γ-ray cured Si–C–N filaments pyrolysed at (a) 1400 °C under nitrogen, (b) 1600 °C under nitrogen and (c) 1400 °C under argon. Sputtering rate 5 nm min^{-1} (reference Ta_2O_5).

carbon (its composition being rather close to that of SiC) (Fig. 5c).

3.3. Morphology, structure and microstructure

In the green state and after the γ-ray curing, the PCSZ-II filaments are almost perfectly cylindrical with a diameter close to 25 μm. During the successive steps of the pyrolysis, both a diameter shrinkage and a density increase occur, as a result of the evolution of gaseous species (i.e. mainly CH_4 and hydrogen). For $\theta_p = 1400\,°C$, the density of the filament is close to 2.47 g cm^{-3} and its diameter equal to about 16 μm, whatever the pyrolysis atmosphere is (Table II).

As shown in Fig. 6, the failure surfaces of filaments submitted to pyrolysis at temperatures ranging from 1200 to 1600 °C under nitrogen or argon exhibit the typical features of brittle materials (including a mirror area and surface defects) responsible for the failure initiation.

The filaments treated at $\theta_p = 1200$ and 1400 °C for 15 min under nitrogen show TEM dark-field images (2 2 0 SiC and 3 1 1 SiC DF) composed of bright diffuse spots and some diffuse SAD patterns (Fig. 7). A through-focus series was undertaken but was not convincing enough to demonstrate any crystallization. For a treatment of 1 h at 1400 °C under the same conditions, TEM dark-field images showed bright spots, and SAD of β-SiC was observed. The average crystallite size is about 5 nm (Fig. 8).

At higher temperature ($\theta_p = 1600\,°C$) for a treatment of 15 min under nitrogen, a SAD pattern of β-SiC was observed. Dark-field images (2 2 0 SiC and 3 1 1 SiC DF) gave an average crystallite size of 7 nm (Fig. 9).

3.4. Mechanical characteristics

The variations of the failure tensile stress and Young's modulus (at room temperature) of Si–C–N filaments, as a function of the highest temperature θ_p achieved during pyrolysis (under nitrogen), are shown in Fig. 10. The failure stress undergoes a maximum

TABLE II Main characteristics of ex-PCSZ γ-ray cured Si–C–N filaments after pyrolysis under nitrogen atmosphere

		θ_p (°C)		
	As spun	1000	1400	1600
Weight loss (%)	–	≈20	< 21	< 21
Composition	$SiC_{1.22}N_{0.45}H_{4.2}O_{0.03}$	$SiC_{0.93}N_{0.46}O_{0.05}$	$SiC_{0.93}N_{0.46}O_{0.05}$	$SiC_{0.98}N_{0.48}O_{0.05}$
Diameter (μm)	≈25	17	16	16
Density (g cm^{-3})			2.47	2.56
State of crystallization	–	Amorphous	Amorphous	Amorphous β-SiC (7 nm)

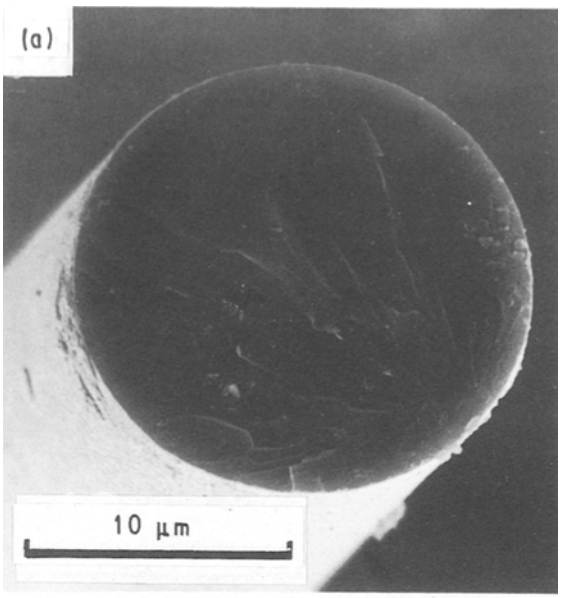

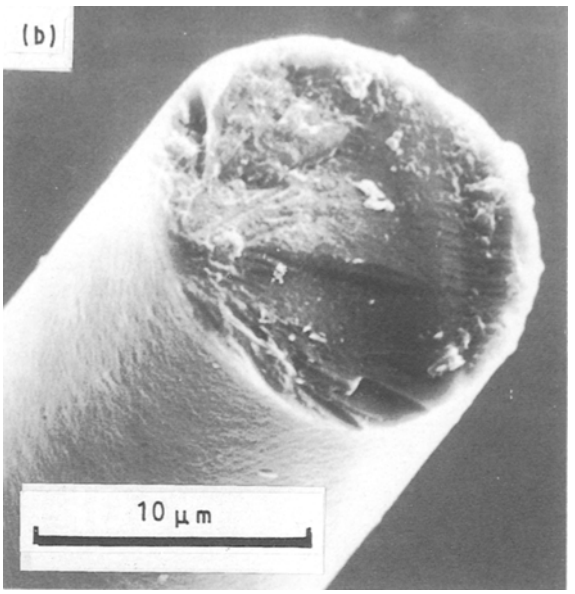

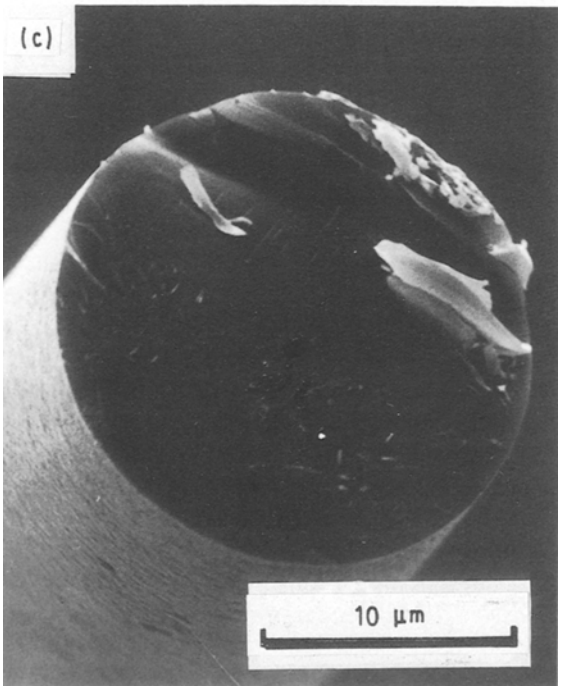

Figure 6 Failure surfaces of ex-PCSZ-II γ-ray cured Si–C–N filaments treated either under nitrogen at (a) 1200 °C and (b) 1600 °C or (c) under argon at 1400 °C.

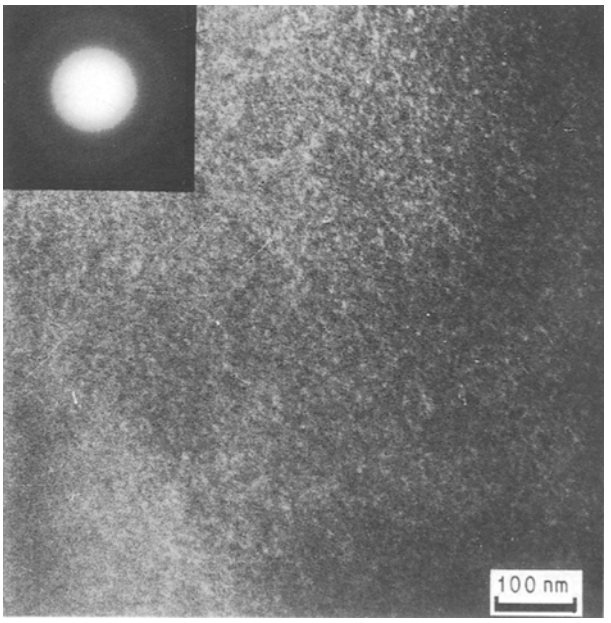

Figure 7 TEM dark-field image of an ex-PCSZ-II γ-ray cured Si–C–N filament after pyrolysis under nitrogen atmosphere at θ_p = 1400 °C for 15 min (the SAD pattern is shown in the insert).

(close to 2500 MPa) for θ_p close to 1200 °C, then it slightly decreases as θ_p is raised from 1200 to 1600 °C. It is noteworthy that the failure stress of the related Si–C–N–O filaments (i) exhibited a lower value for θ_p = 1200 °C (i.e. about 1900 MPa) and moreover (ii) was observed to fall by 30% when θ_p was raised to 1400 °C [39]. The Young's modulus increases from 185 to 214 GPa when θ_p is raised from 1000 to 1200 °C, then it increases more slowly and is equal to 220 GPa for θ_p = 1600 °C.

When treated under argon, the Si–C–N filaments exhibit lower mechanical properties than their counterparts which have been treated under nitrogen. Thus, for θ_p = 1400 °C, their tensile failure stress at room temperature is only equal to 1900 MPa (instead of ~ 2300 MPa for the filaments pyrolysed under nitrogen).

4. Discussion

The data which have been reported in section 3 show that PCSZ-II, an oxygen-free precursor to Si–C–N ceramics resulting from the co-polymerization of dichlorodimethylsilane and 1.3-dimethyl-1.3-dichlorodisilazane, can be cured by γ-ray irradiation in the absence of oxygen. As can be seen from Fig. 2, a low irradiation dose already has a very pronounced effect on the hexane-insoluble fraction and ceramic yield, a feature which supports the occurrence of a transition from a poorly crosslinked polymeric structure to a three-dimensional framework. Such a transition, induced by γ-rays, has already been mentioned

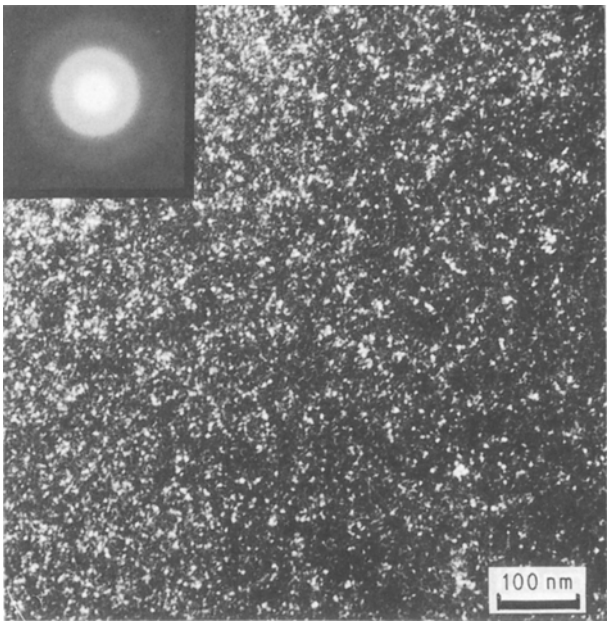

Figure 8 TEM dark-field image of an ex-PCSZ-II γ-ray cured Si–C–N filament after pyrolysis under nitrogen atmosphere at θ_p = 1400 °C for 1 h (the SAD pattern is shown in the insert).

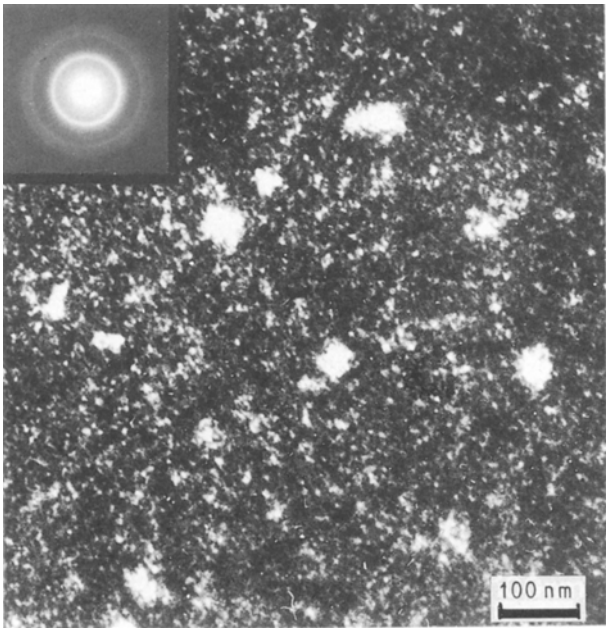

Figure 9 TEM dark-field image of an ex-PCSZ-II γ-ray cured Si–C–N filament which has been treated under nitrogen at 1600 °C, the aperture being in position 2 (the SAD-pattern is shown in the insert).

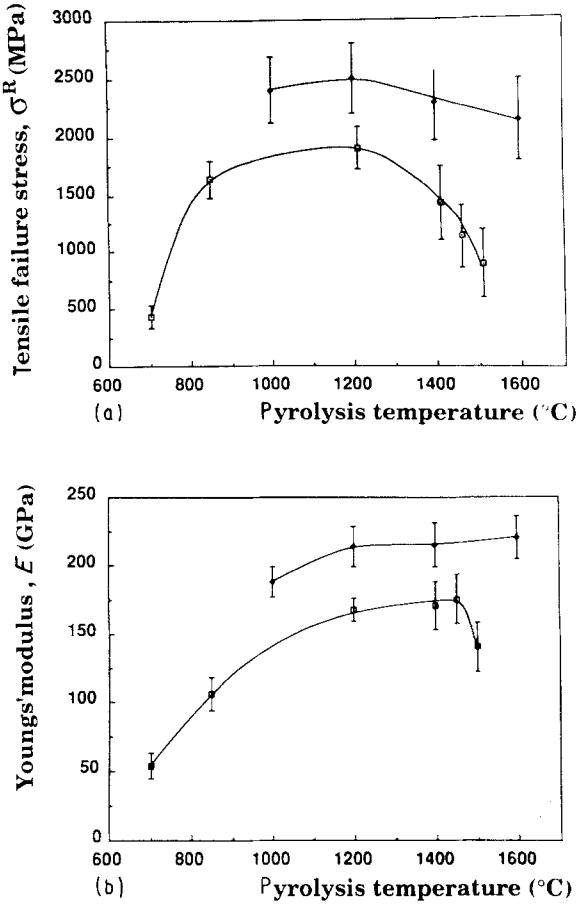

Figure 10 Mechanical properties at room temperature of ex-PCSZ (◆) Si–C–N (γ-ray cured) and (⊡) Si–C–N–O (oxygen-cured) filaments pyrolysed under nitrogen atmosphere at increasing temperatures θ_p: (a) tensile failure stress, (b) Young's modulus.

by different authors [43–47] in organosilicon polymers and more recently by Taki *et al.* [45, 46] in polycarbosilanes. The detailed mechanism which is actually involved in the curing process of PCSZ-II by γ-rays in the absence of oxygen is still unknown. However, it might be close to that reported by Okamura [36] in a study of the curing of PCS, which was shown to involve the formation of free radicals (i.e. $-\dot{C}H-Si(CH_3)_2$; $-CH_2-\dot{S}i(CH_3)_2$ and $-\dot{C}H-SiH(CH_3)$ –) and hydrogen (and to a lesser extent methane). It can be assumed that formation and coupling of free radicals afford the three-dimensional polymeric framework. In the present work, hydrogen was also observed to be formed during the γ-ray irradiation of PCSZ-II (as evidenced by the analysis of the gas content of the sample containers after irradiation). We suggest that the free radicals formed during the irradiation process could be as follows:

$$\begin{array}{cccccc} C-\dot{S}i-C & Si-\dot{C}-Si & -\dot{S}i- & Si-\dot{N}-H & Si-\dot{N}-Si \\ | & | & | & & \\ N & H & Si & & \end{array}$$

Experimental studies of the nature of the free radicals, their respective lifetimes as well as the correlation between the formation of the free radicals and the curing process mechanism, are in progress in our laboratories.

As shown in Fig. 2, the variations of both the hexane-insoluble fraction τ_i and ceramic yield η as a function of the irradiation dose are not smooth, a feature which suggests that the formation of the various free radicals depends on the irradiation dose value. The occurrence of a pronounced increase in both τ_i and η as the irradiation dose is raised within the range 0–150 Mrad could be explained by (i) the easy formation of some radicals as mentioned above, and (ii) the fast coupling reaction between these radicals made possible by the proximity of the sites where they have been formed. Otherwise, the second parts of

the curves with weak slopes corresponding to a slow increase of τ_i and η with irradiation dose might be related to a substantial increase of viscosity and concomitant decrease of the coupling aptitude of radicals.

On the basis of the data reported in section 3 and of the conclusions previously drawn in parts I–III, the pyrolysis of oxygen-free PCSZ-II filaments, spun in the molten state and cured without oxygen by means of γ-rays (irradiation dose 350 Mrad), as well as their main properties, can be discussed as follows:

(i) For $25 < \theta_p < 450\,^{\circ}C$, a first weight loss is observed (Fig. 4) which is mainly assigned to an evolution of oligomers. The fact that its value is low (i.e. 10%), with respect to that (i.e. 23%) corresponding to the uncured PCSZ-II, shows that the γ-ray curing process is effective. As a matter of fact, in a three-dimensional polymeric framework, the polymeric chain ends have disappeared, a feature which makes the release of oligomers much more difficult as previously pointed out by several authors for related materials [46, 47].

(ii) For $450 < \theta_p < 850\,^{\circ}C$, a second weight loss (of the order of 10%) occurs which can be assigned to the organic–inorganic transition, on the basis of the results of our study of the pyrolysis of bulk PCSZ samples [37]. It is known to result in an evolution of hydrogen and methane, on the one hand, and an important filament diameter shrinkage, on the other hand (Table II). For $\theta_p = 850\,^{\circ}C$ the filaments consist of an amorphous Si–C–N material whose formula is close to $SiC_{0.93}N_{0.46}$ and its oxygen concentration less than 2 wt %. Furthermore, it is thought that the Si–C–N amorphous material contains also a small amount of hydrogen, as established for the bulk Si–C–N samples in part I [37].

(iii) For $850 < \theta_p < 1400\,^{\circ}C$, the amorphous Si–C–N material undergoes only minor change. Its chemical composition remains stable (Table II) with the exception of a possible release of residual hydrogen which is responsible for a small weight loss and diameter shrinkage, whatever the nature of the pyrolysis atmosphere (i.e. argon or nitrogen). The high thermal stability of the amorphous Si–C–N filaments with respect to their Si–C–O counterparts is thought to be related to (i) the occurrence of a high concentration of nitrogen heteroatoms (playing a role similar to that of oxygen) and (ii) the absence of early decomposition processes releasing gaseous oxides (SiO and CO), both phenomena impeding the formation of SiC_4 sites and subsequently the growth of β-SiC crystals. It is noteworthy that a similar conclusion has been previously drawn for the Si–C–N–O filaments [39] which also remain amorphous up to about the same temperature, a feature which emphasizes the stabilizing effect of nitrogen and its beneficial role in such materials. Within the temperature range $1000 < \theta_p < 1400\,^{\circ}C$ (Fig. 10) the tensile failure stress σ^R (which undergoes a broad maximum for $\theta_p = 1200\,^{\circ}C$) is higher than that previously reported in part III [39] for the Si–C–N–O filaments whatever θ_p is. This feature suggests that the flaws formed in the filaments during the pyrolysis process are less severe when the filaments have been cured by γ-ray irradiation. Within the same temperature range, the Young's modulus increases from 190 to 215 GPa, probably due to the release of hydrogen and the related densification process of the amorphous material, as already mentioned. The lower stiffness observed for the Si–C–N–O filaments is thought to be related to the occurrence of a large amount of Si–O bonds (the Young's modulus of silica itself being close to 75 GPa, increasing the oxygen concentration in ex-PCSZ filaments should lower their stiffness). Finally, the Young's modulus of Si–C–N filaments, although it is significantly higher than those reported previously for the related Si–C–O and Si–C–N–O filaments, remains far from that of Si_3N_4 and SiC CVD filaments ($E \approx 400$–450 GPa for SiC), a feature which might be due to both their amorphous structure and the occurrence of a significant porosity at the nanometre scale (the density of Si–C–N amorphous filaments is only 2.5 $g\,cm^{-3}$ for $\theta_p = 1400\,^{\circ}C$ whereas that of CVD SiC is 3.2 $g\,cm^{-3}$).

(iv) For $1400 < \theta_p < 1600\,^{\circ}C$, the microstructure of the filaments depends on both the value of θ_p and the nature of the pyrolysis atmosphere. When the pyrolysis is performed under argon, the filaments undergo a decomposition process in the vicinity of their surface which is already apparent for $\theta_p = 1400\,^{\circ}C$ (it might even start at somewhat lower temperatures) (Fig. 5c). This decomposition process results in the formation of a skin, depleted in both silicon and nitrogen and thus enriched in carbon. Even under such unfavourable conditions the thermal stability of the amorphous Si–C–N filaments is much higher than that of the ex-PCS Si–C–O fibres commonly used in CMCs and which are known to undergo a decomposition–crystallization process at temperatures as low as 1100–1200 °C. Conversely, when the pyrolysis is performed under nitrogen at the same temperature ($\theta_p = 1400\,^{\circ}C$), almost no decomposition takes place near the filament surface, as shown in Fig. 5a. Therefore and as expected, the thermal stability of the amorphous Si–C–N filaments appears to be higher under nitrogen-rich atmospheres than under argon.

Interestingly, the overall elemental composition of the Si–C–N filaments which have been cured without oxygen and pyrolysed under pure nitrogen was observed to remain almost unchanged when θ_p is raised from 1000 °C to values as high as 1600 °C. Such a stability has never been reported for an ex-organosilicon fibrous material, as far as we know. However, the AES and TEM studies reported in section 3 have shown that local structural and microstructural changes actually occur in the filaments as θ_p is raised from 1400 to 1600 °C, which in turn results in a slight decrease in σ^R and increase in E at room temperature (Fig. 10).

On the one hand, a thin skin (apparent thickness 50 nm) is formed at the filament surface, which is clearly apparent for $\theta_p = 1600\,^{\circ}C$ (Fig. 5b). Since it consists of almost pure carbon (at least in the very vicinity of the filament surface), it might result from a thermal decomposition of the ternary Si–C–N amorphous material with simultaneously a release of

nitrogen and gaseous Si-based species (not to say silicon itself). Thus it is suggested that such a decomposition process, if it ever takes place *in situ* in a CMC, would probably not embrittle the material in as much as this carbon layer growing at the fibre surface would come in addition to the initial interphase material (e.g. carbon). A similar decomposition process is known to occur actually in CMCs elaborated from ex-PCS Si–C–O fibres (Nicalon fibres from Nippon Carbon) [48]. However, the main difference between the Si–C–N filaments studied here and ex-PCS Si–C–O fibres lies in the fact that the decomposition process responsible for the formation of carbon takes place at a temperature which is lower for the latter (i.e. 1100–1200 °C) and falls within the temperature range at which some CMCs are actually processed (e.g. hot pressing for SiC (ex-PCS) glass–ceramics).

On the other hand, when θ_p is raised from 1400 to 1600 °C or the duration is raised from 15 min to 1 h at 1400 °C, β-SiC crystals are formed within the Si–C–N amorphous matrix (Figs 8 and 9). Their mean size (which is of the same order, i.e. a few nanometres, as that observed for the Si–C–N–O filaments treated under nitrogen at the same temperature) is much lower than those measured either for Si–C–O or Si–C–N–O filaments (respectively 200 and 15–20 nm) treated under argon at 1600 °C [39, 49].

Finally, the absence of any pronounced drop in the mechanical properties at 25 °C of Si–C–N filaments cured without oxygen and pyrolysed under pure nitrogen for θ_p ranging from 1200 to 1600 °C appears to be rather new in the field of ex-organosilicon fibrous materials: (i) the Young's modulus remains constant (it even slightly increases) and (ii) the decrease in tensile failure stress is only 15% (with respect to the maximum for $\theta_p = 1200$ °C), σ^R being still equal to 2100 MPa for $\theta_p = 1600$ °C (Fig. 10). The difference between the dependence on θ_p of the mechanical behaviour of Si–C–N–O and Si–C–N filaments pyrolysed at very high temperatures under nitrogen might be mainly related to the absence of any thick decomposition skin for the oxygen-free filaments. This feature emphasizes the detrimental effect of oxygen on the thermal stability and thus the mechanical properties of ex-PCSZ filaments.

5. Conclusion

From the experimental data reported in section 3 and the discussion in section 4, the following conclusions can be drawn:

(i) Si–C–N model filaments, almost free of oxygen and about 16 μm in diameter, have been prepared for the first time from a new PCSZ precursor, by melt-spinning, γ-ray curing and pyrolysis under nitrogen (or argon) at a temperature as high as 1600 °C.

(ii) The amorphous filaments resulting from the organic–inorganic conversion of the precursor exhibit a composition close to $SiC_{0.93}N_{0.46}$ (with less than 2 wt % of oxygen) and undergo only minor change in composition and structure up to about 1400 °C either under argon or nitrogen.

(iii) When heated under argon beyond 1400 °C, they undergo a decomposition process which starts from the filament surface, yielding a skin enriched in C and depleted in both Si and N. However, the kinetics of growth of this skin is much slower than that reported for ex-PCS fibres commonly used in many CMCs.

(iv) Si–C–N filaments exhibit an exceptionally high stability when heated under nitrogen within the 1400–1600 °C temperature range: the only noticeable phenomena are the formation of a very thin carbon skin and that of tiny β-SiC crystals (mean size 6 nm) within an Si–C–N matrix which remains amorphous.

(v) Si–C–N filaments are characterized at room temperature by high stiffness ($E \sim 220$ GPa) and tensile failure stress ($\sigma^R \sim 2400$ MPa) which remain almost constant after ageing treatments under nitrogen at 1400–1600 °C. It is thought that the failure stress could be further increased by reducing the filament diameter.

Furthermore, a comparison between the properties of the Si–C–N (present work) and Si–C–N–O [39] filaments processed from the same PCSZ-II precursor shows that both oxygen and nitrogen heteroatoms stabilize the amorphous structure resulting from the organic–inorganic transition, by impeding the formation of some $\underline{Si}C_4$ sites and subsequently the growth of β-SiC crystals, on the one hand, and oxygen has a detrimental effect on the stability of the amorphous state at high temperatures, promoting its decomposition by formation of SiO and CO species, on the other hand. Thus, oxygen-free Si–C–N fibres might be a better reinforcement at high temperatures than the presently used Si–C–O fibres.

Acknowledgements

This work was done within the framework of a national programme involving CNRS, the Ministry of Defence (DRET), Rhône-Poulenc (RP) and SEP, whose support is acknowledged. The authors are indebted to P. Olry from SEP and O. Caix and E. Chassagneux from RP for their interest in the present work and valuable discussions.

References

1. C. T. LYNCH and J. P. KERSHAW (eds), "Metal Matrix Composites" (Chemical Rubber Co./CRC Press, Cleveland, 1972) p. 15.
2. L. J. BROUTMAN and R. H. KROCK, in "Composite Materials", Vol. 4: "Metallic Matrix Composites", edited by K. G. Kreider (Academic Press, New York, 1974) p. 1.
3. R. NASLAIN, in "Introduction to Composite Materials", Vol. 2, "Metallic and Ceramic Matrix Composites" (in French) (CNRS/IMC, Bordeaux, 1985) p. 19.
4. D. C. PHILLIPS, *Compos. Sci. Tech.* **40** (1991) 1.
5. J. R. STRIFE, J. J. BRENNAN and K. M. PREWO, *Ceram. Eng. Sci. Proc.* **11** (7.8) (1990) 871.
6. R. WARREN, in "Research and Developments of High Temperature Materials for Industry", edited by E. Bullock (Elsevier Applied Science, London, 1989) p. 169.
7. A. K. DHINGRA, *Phil. Trans. R. Soc. London A* **294** (1980) 411.
8. D. D. JOHNSON, A. R. HOLTZ and M. F. GRETHER, *Ceram. Eng. Sci. Proc.* **8** (1980) 744.

9. T. I. MAH, M. G. MENDIRATTA, A. P. KATZ and K. S. MEZDIYASNI, *Ceram. Bull.* **66** (1978) 304.
10. D. B. MARSHALL, F. F. LANGE and P. D. MORGAN, *J. Amer. Ceram. Soc.* **70** (8) (1987) 187.
11. J. B. DONNET and R. C. BANSAL, in "Carbon Fibers" Dekker, (New York, 1984) p. 1.
12. D. R. LOWELL, in "Carbon Fibers Technology Uses and Prospects" (Plastics and Rubber Institute/Noyes Publications, London, 1986) p. 39.
13. S. YAJIMA, K. OKAMURA, T. MATSUZAWA, Y. HASEGAWA and T. SHISHIDO, *Nature* **279** (1979) 706.
14. S. YAJIMA, Y. HASEGAWA, J. HAYASHI and M. IIMURA, *J. Mater. Sci.* **13** (1978) 2569.
15. Y. HASEGAWA, M. IIMURA and S. YAJIMA, *ibid.* **15** (1980) 720.
16. K. OKAMURA, US Patent 4 650 773 17 (1987).
17. S. YAJIMA, J. HAYASHI and M. OMORI, *Chem. Lett.* (1975) 931.
18. *Idem, ibid.* (1975) 1209.
19. T. J. CLARK, M. JAFFE, J. RABE and N. R. LANGLEY, *Ceram. Eng. Proc.* **7** (7-8) (1986) 901.
20. K. OKAMURA, *Composites* **18** (2) (1987) 107.
21. K. OKAMURA, M. SATO and T. MATSUZAWA, *Amer. Ceram. Soc. Polym. Prepr.* **25** (1) (1984) 6.
22. L. C. SAWYER, R. T. CHEN, F. HAIMBACK, P. J. HARGET, E. R. PRACK and M. JAFFE, *Ceram. Eng. Sci. Proc.* **7** (1986) 914.
23. T. MAH, N. L. HECHT, D. E. McCULLUM, J. R. HOENIGMAN, H. M. KIM, A. P. KATZ and H. A. LIPSITT, *J. Mater. Sci.* **19** (1984) 1191.
24. K. OKAMURA, M. SATO, Y. HASEGAWA, in Materials Science Monographs, Vol. A, "High Tech Ceramics", edited by P. Vincenzini (Elsevier Science, Amsterdam, 1987) p. 747.
25. Y. NAKAIDO, Y. OTANI, N. KOZAIKAI and J. OTANI, *Chem. Lett.* (1987) 705.
26. B. G. PENN, J. G. DANIELS, F. E. LEDBETTER III and J. M. CLEMONS, *SAMPE Q.* **15** (1984) 39.
27. E. BOUILLON, D. MOCAER, J. F. VILLENEUVE, R. PAILLER, R. NASLAIN, M. MONTHIOUX, A. OBERLIN, C. GUIMON and G. PFISTER, *J. Mater. Sci.* **26** (1991) 1517.
28. S. M. JOHNSON, R. D. BRITTAIN, R. H. LAMOREAUX and D. J. ROWCLIFFE, *J. Amer. Ceram. Soc.* **71** (3) (1988) 132.
29. K. L. LUTRA, *ibid.* **69** (10) (1986) C 321.
30. K. M. PREWO and J. J. BRENNAN, *J. Mater. Sci.* **17** (1982) 1201.
31. K. M. PREWO, *ibid.* **21** (1986) 3590.
32. R. CHAIM and A. H. HEUER, *Adv. Ceram. Mater.* **2** (2) (1987) 154.
33. G. E. LEGROW, T. F. LIM, J. LIPOWITZ and R. S. REAOCH, *Ceram. Bull.* **66** (2) (1987) 363.
34. G. PEREZ and O. CAIX, in "Proceedings of 4th European Conference on Composite Materials (ECCM 4), edited by J. Füller, G. Gruninger, K. Schulte, A. R. Bunsell and A. Massiah (Elsevier Applied Science, London, 1990) p. 573.
35. K. OKAMURA, M. SATO, T. SSEGUCHI and S. KAWANISHI, in Controlled Interfaces in Composite Materials, edited by H. Ishida, (Elsevier Science New York, 1990) p. 209.
36. K. OKAMURA in Proceedings of 7th CIMTEC World Ceramic Congress and Satellite Symposium, edited by P. Vincenzoni (Elsevier Science, Amsterdam, 1991) p. 19.
37. D. MOCAER, R. PAILLER and R. NASLAIN, *J. Mater. Sci.* **28** (1993) 2615.
38. *Idem, ibid.* **28** (1993) 2632.
39. *Idem, ibid.* **28** (1993) 2639.
40. E. BACQUE, J. P. PILLOT, J. DUNOGUES and P. OLRY, Brevet Européen 296 028 (1988).
41. K. SHIINA and M. KUMADA, *J. Org. Chem.* **23** (1958) 139.
42. A. R. BUNSELL, J. W. S. HEARLE and R. D. HUTER, *J. Phys. E (Sci. Instrum).* **4** (1971) 868.
43. J. KO and J. MARK, *Macromolecules* **8** (1975) 869.
44. B. I. LEE and R. L. HENCH, in "Science of Ceramic Chemical Processing", edited by L. L. Hench and D. R. Ulrich (Wiley-Interscience, New York, 1986) p. 345.
45. T. TAKI, K. OKAMURA and M. SATO, *J. Mater. Sci.* **24** (1989) 1263.
46. T. TAKI, K. OKAMURA, M. SATO, T. SEGUCHI and S. KAWANISHI, *J. Mater. Sci. Lett.* **7** (1988) 209.
47. R. WEST, L. D. DAVID, P. I. DJUROVICH, H. YO and R. SINCLAIR, *Ceram. Bull.* **62** (1983) 916.
48. C. COJEAN, M. MONTHIOUX and A. OBERLIN, in Proceedings of 7th National Day on Composite Materials, edited by G. Fantozzi and P. Fleischmann (1990) p. 381.
49. O. DELVERDIER, M. MONTHIOUX and A. OBERLIN, *ibid.* p. 391.

Received 20 July
and accepted 11 August 1992